Published in final edited form as:
Exp Gerontol. 2013 December ; 48(12): . doi:10.1016/j.exger.2013.10.003.

Ventromedial PFC, Parahippocampal, and Cerebellar Connectivity Are Associated with Temporal Discounting in Old Age

S. Duke Han[1,2,6], **Patricia A. Boyle**[1,2,3], **Lei Yu**[2,3], **Debra A. Fleischman**[1,2,3], **Konstantinos Arfanakis**[2,4,5], and **David A. Bennett**[2,3]

[1]Department of Behavioral Sciences, Rush University Medical Center, Chicago, IL 60612

[2]Rush Alzheimer's Disease Center, Rush University Medical Center, Chicago, IL 60612

[3]Department of Neurological Sciences, Rush University Medical Center, Chicago, IL 60612

[4]Department of Biomedical Engineering, Illinois Institute of Technology, Chicago, IL 60616

[5]Department of Radiology, Rush University Medical Center, Chicago, IL 60612

[6]Mental Health Care Group, VA Long Beach Healthcare System, Long Beach, CA 90822

Abstract

Temporal discounting occurs when a greater delayed reward is forsaken for a smaller immediate reward, and has been associated with a number of financial and health care outcomes important for older adults. Using resting-state fMRI and seed regions of interest in the left and right fronto-insular (FI) cortex, we explored the neurobiological substrate of temporal discounting in 123 non-demented older adults from the Rush Memory and Aging Project. For the left FI, temporal discounting was positively associated with functional connectivity to the right ventromedial prefrontal cortex and middle temporal regions, and negatively associated with parahippocampal and right cerebellar regions. For the right FI, temporal discounting was negatively associated with functional connectivity to a right cerebellar region. Connectivity maps of both left and right seed regions of interest overlapped in the right cerebellum. Results support the notion of different brain functional connectivity patterns associated with the dynamic range of temporal discounting in old age.

Keywords

Temporal discounting; aging; functional connectivity; fronto-insular cortex; ventromedial prefrontal cortex

Contact information: S. Duke Han, PhD, ABPP-CN, Rush Alzheimer's Disease Center, 600 S. Paulina St., Suite 1022, Chicago, IL 60612, Duke_Han@rush.edu, Phone: 312-942-2028, Fax: 312-563-4605.

Conflict of Interest

The authors declare no competing financial interests.

Introduction

Temporal discounting refers to when individuals prefer a smaller, more immediate reward versus a larger reward at a later time. The greater value of the delayed reward is "discounted" for the more immediate smaller reward. Temporal discounting is believed to reflect a type of impulsivity or a difficulty in considering future events in decision making (Ainslie, 1975) and has been associated with many meaningful real-word phenomena such as drug addiction (Bickel et al., 2007), weight gain in obesity (Kishinevsky et al., 2012), and credit card debt (Meier and Sprenger, 2010). Temporal considerations are significant factors in decisions that are associated with financial and health wellbeing of older adults and their families.

Understanding the neurobiologic substrate of temporal discounting is a significant public health concern since this is a necessary step to the development of interventions that promote effective decision making and well being in old age. While there have been some studies of temporal discounting in younger populations (McClure et al., 2004; 2007; Hariri et al., 2006; Cardinal, 2001), very little is known of the neural mechanisms of temporal discounting in old age. A neuroimaging method that may assist in elucidating the neurobiological substrates of this complex behavioral characteristic is resting-state fMRI (rs-fMRI). This noninvasive approach ascertains functional connectivity parameters in brain networks through temporal coherence of low frequency fluctuations in the blood-oxygenation-level-dependent (BOLD) signal among brain regions. Regions that demonstrate high temporal coherence are believed to function as a network, and the strength of the connections within these networks may vary according to multiple factors. This brain imaging approach is brief, requires little to no cognitive engagement on the part of the participant, and has been successfully used to illuminate complex mechanisms of the dementia process (Greicius et al., 2004; Buckner et al., 2005). This approach has been recently used to study temporal discounting in a young adult population (Li et al., 2013); however, to our knowledge, this approach has not been used to examine temporal discounting in old age.

Using resting-state fMRI, we explored the neurobiological substrate of temporal discounting in 123 non-demented older adults from the Rush Memory and Aging Project, a longitudinal and community-based cohort study of aging. All participants underwent extensive clinical assessments and behavioral economic questions that assessed for temporal discounting. For our functional connectivity analyses, we utilized the fronto-insular cortex (right and left) as our seed region of interest for three reasons: (1) it has been considered critical in studies of value-assessments and social decision making due to the proliferation of spindle neurons in this region (Allman et al., 2010), (2) it has been shown to be active during discounting tasks regardless of response (Whittman et al., 2010), suggesting it has an important role in decision making regardless of type of choice, and (3) it has been previously used to interrogate the functional network of frontal regions that have been heavily implicated in studies of temporal discounting (Seeley et al., 2007). Based on previous task-related fMRI and brain lesion studies of temporal discounting in younger populations, we hypothesized that functional connectivity to the ventromedial prefrontal cortex region would show a positive association to temporal discounting (McClure et al., 2004; 2007).

Methods

Participants

All procedures were approved by an Institutional Review Board at Rush University Medical Center. Participants for this study were 123 older adults without dementia and were individuals enrolled in the Rush Memory and Aging Project, a community-based cohort

study of aging and dementia (Bennett et al., 2012). Study participants in the Rush Memory and Aging Project were recruited from local residential facilities, including retirement homes, senior housing facilities, and community organizations in the Chicago metropolitan area. All participants were without known dementia when they were enrolled, and they are followed annually. For the current study, inclusion criteria required that participants be without dementia based on a detailed clinical evaluation (Bennett et al., 2006). Cognitive impairment was determined by a clinical neuropsychologist with expertise in aging and AD who reviewed the cognitive data, information about the participant's background (e.g., education/occupation, sensory and motor deficits), and a clinical evaluation of the participant done by a clinician with expertise in aging and dementia. A diagnosis of dementia was determined in accordance with NINCDS/ADRDA criteria by the evaluating clinician (Bennett et al., 2002; Boyle et al., 2005).

The Memory and Aging Project began in 1997 and assessment of discounting and brain imaging were initiated in 2008. At the time of these analyses, 1299 participants had enrolled and completed their baseline evaluation in the parent study, 443 died, and 77 refused further participation before discounting and scan data collection began. Of the remaining 779, 260 had MRI contraindications or were unable to sign informed consent leaving 519 eligible for scanning. Of these, 155 (29.9%) refused, 214 were scanned, and the remaining 150 were still being scheduled for scanning. From the 214 that were scanned, 14 were dropped due to excessive motion, 7 were dropped due to scanning data acquisition problems, leaving 193 participants. An additional 9 participants were dropped because of quality assurance issues relating to scan data, leaving 184 participants. Sixty-one participants of the remaining 184 were not given temporal discounting behavioral assessments at the time of analysis, leaving 123 participants without dementia who had undergone neuroimaging and completed temporal discounting behavioral economic assessments.

Assessment of Temporal Discounting

Temporal discounting was assessed using 7 binary questions, following a standard preference elicitation protocol, as described in detail previously (Boyle et al., 2012). Participants were asked to choose between an immediate, smaller or a delayed, larger payment. An example is: "Which do you prefer, that you get $10 in cash right now or $13.50 in a month?" The current payoff was fixed at $10 and the delay period was fixed at one month for all questions. Delayed payments ranged from $10.75 to $30, with payment amounts varying across questions.

Image Acquisition and Processing

The mean time period between temporal discounting and neuroimaging was approximately 6 months (mean days=174.63, standard deviation days=196.02). Magnetic resonance imaging (MRI) scans were conducted on a 1.5 Tesla clinical scanner (General Electric, Waukesha, WI), equipped with a standard quadrature head coil, located within the community of the sample. High data quality was ensured through daily tests of the scanner's performance and thorough quality control tests on the raw data. High-resolution T1-weighted anatomical images were collected with a 3D magnetization-prepared rapid acquisition gradient-echo (MPRAGE) sequence with the following parameters: TR = 6.3 ms; TE = 2.8 ms; preparation time = 1000 ms; flip angle = 8°; 160 sagittal slices; 1 mm slice thickness; field of view (FOV) = 24 cm × 24 cm; acquisition matrix 224 × 192, reconstructed to a 256 × 256 image matrix; scan time = 10 min and 56 secs. Two copies of the T1-weighted data were acquired on each subject and averaged. Resting state MRI data was acquired using a 2D spiral in/out echo-planar imaging (EPI) sequence with the following parameters: TR = 2000 ms; TE = 33 ms; flip angle = 85°; 26 oblique axial slices; 5 mm slice thickness; acquisition/

reconstruction matrix 64 × 64; FOV = 24 cm × 24 cm; 240 time-points/volumes; scan time = 8 min. Participants were asked to keep their eyes closed.

The skull was removed from the averaged structural MRI data using FreeSurfer'sHybrid Watershed Algorithm (Segonne et al., 2004). Structural scans were also manually edited when necessary to remove residual non-brain material. Brain segmentation into gray matter, white matter and CSF was also performed using FreeSurfer (http://surfer.nmr.mgh.harvard.edu/). Whole brain volume was derived, and the portion of brain volume occupied by each tissue type was calculated. The first 6 image volumes of resting state data were discarded to avoid using data collected before reaching MRI signal equilibrium. Images were reconstructed on Linux machines from the acquired k-space data (Glover et al., 2004). Using the Statistical Parametric Mapping software (Friston et al., 1995; http://www.fil.ion.ucl.ac.uk/spm/) version 8 (SPM8), all volumes were corrected for slice-timing and motion, were co-registered to the corresponding high-resolution T1-weighted data using affine transformation, and spatially normalized to the Montreal Neurological Institute (MNI) template. The normalized image volumes were spatially smoothed with a 7mm full-width half-maximum (FWHM) Gaussian kernel. Next, a bandpass filter of 0.01 to 0.08 Hz was applied to the data in temporal frequency space to minimize low-frequency signal drift and high frequency signal variations due to cardiac and respiratory effects. In order to remove any residual effects of motion and other non-neuronal factors, 6 head motion parameters, as well as parameters for the white matter signal, global mean signal, and cerebrospinal fluid signal were used as nuisance variables (Buckner et al., 2009) in functional connectivity analysis using the Data Processing Assistant for Resting-State fMRI (DPARSF; http://restfmri.net/forum/DPARSF) and SPM8.

To address concerns of head motion, we employed a two-step process of exclusion. All of the participants included in the study had to satisfy exclusion criteria of head movement during the entire fMRI scanning session of less than 2.5mm translation in any axis and less than 2.5° angular rotation in any axis. They also had to satisfy an additional head movement exclusion of 1.9mm translation in any axis and less than 1.9° angular rotation in any axis over any 10 second interval.

Assessment of Cognition

All participants underwent neuropsychological evaluation. Participants were administered a battery of neuropsychological tests. These included the Word List Memory, Word List Recall, and Word List Recognition from the CERAD battery, the immediate and delayed recall of Logical memory Story A and the East Boston Story, Verbal Fluency, Boston Naming Test, a subset of items from the Complex Ideational Material Test, the National Adult Reading Test, Digit Span subtest (forward and backward) of the Wechsler Memory Scale-Revised, Digit Ordering, the Symbol Digit Modalities Test, Number Comparison, the Judgment of Line Orientation Test, and Standard Progressive Matrices. A global cognition score was also calculated by averaging the z-scores across all measures of cognitive function.

Statistical Analyses

Temporal Discounting

The approach to determining temporal discounting has been detailed in prior work (Boyle et al., 2012). Briefly, the discounting factor α was estimated using an established hyperbolic function (Laibson, 1997; Frederick et al., 2002; Kirby et al, 1999; Kirby, 1997):

$$V=\frac{A}{1+\alpha D} \quad (1)$$

where V represents the magnitude of the discounted value of the future reward A at delay D. Larger values of V correspond to smaller values of α.

If the observed outcome of a trial is represented by Y, the decision to choose a later reward is represented by Y = 1, and the decision to choose a current reward is represented by Y = 0, we hypothesized that the probability P(Y = 1) depends on the difference between the discounted future reward V and the present reward C. Therefore the odds of choosing future reward over present reward can be expressed as:

$$\frac{P(Y=1)}{P(Y=0)}=e^{V-C} \quad (2)$$

For example, if V-C=0, this would represent no difference between the delayed and current rewards. If V - C is positive, this would represent a predilection for the delayed reward with odds greater than 1. A negative V - C would represent a predilection for the immediate reward. The discounting rate α could therefore be derived from equation (2).

The Chronbach's alpha of the temporal discounting measure was 0.86, indicating adequate internal consistency. Further, because there are different ways of estimating discounting, an exponential function that generates k-values was used as a comparison (Boyle et al., 2012). The correlation between the α and k values was 0.99 ($p<0.001$), suggesting both yield comparable measures of discounting.

Functional Neuroimaging

A spherical seed region of interest with a radius of 4mm was prescribed in the fronto-insular cortex, with MNI coordinates of x = 38, y = 26, z = −10 (right FI) in accordance with previous work (Seeley et al., 2007) and x = −38, y = 26, z = −10 (left FI) in consideration of hemispheric laterality. A mean signal time course for each of the seeds was calculated and used as a reference. Analyses were then conducted by examining the partial correlations between the reference signal time course and the time series of each other voxel in the brain. The voxels showing significant functional connectivity to the seed ROIs were identified as those voxels whose partial correlation differed significantly from 0, based on whole-brain Fisher's z-transformation of the correlations at the individual level. In order to interrogate brain regions functionally connected to the seed regions of interest, AlphaSim Monte Carlo simulations (10,000 permutations) as determined by the AlphaSim program in AFNI (http://afni.nimh.nih.gov) were employed to correct for multiple comparisons at cluster $p<0.05$. This corresponded to a cluster size > 39 voxels for a voxel threshold $p<0.004$ for the left FI and the right FI. Next, results of the whole-brain Fisher's z-transformation were then correlated with temporal discounting, while covarying for age, education, sex, and global cognition using the same parameters for correction for multiple comparisons. Age, education, and sex are factors known to correlate with multiple outcomes in epidemiologic studies. Results were also adjusted for global cognition as this has been associated with temporal discounting (Boyle et al., 2012). Seed-based functional connectivity analysis was conducted with Resting-State fMRI Data Analysis Toolkit (REST: http://restfmri.net/forum/REST).

Results

Descriptive data are shown in Table 1. The sample was predominantly white and female with an education beyond high school. Mini-Mental Status Examination (MMSE) score and global cognition scores were within the average range as expected for non-demented older adults. There were no significant associations between temporal discounting and demographic variables. Seeding of the left and right FI yielded similar networks of functionally related regions (Figure 1). Inferior lateral and medial frontal, and superior lateral and medial temporal regions appeared to be particularly with the FI seed ROIs.

Adjusting for age, education, sex, and global cognition, voxel-wise comparisons revealed that temporal discounting was positively associated with functional connectivity between the left FI and a region in the right ventromedial prefrontal cortex, two regions in the right middle temporal cortex, and one region in the left middle temporal cortex. For the left FI, temporal discounting was negatively associated with functional connectivity to the right parahippocampal and right cerebellar regions (Figure 2, Table 2).

Temporal discounting was negatively associated with functional connectivity between the right FI and the right cerebellum (Figure 3).

Separate functional connectivity maps corresponding to seed regions of interest in the left and right FI appeared to overlap at a region in the right cerebellum (Figure 4).

In order to demonstrate the selectivity of our observations, we used four additional 4mm radius seed regions of interest in the motor cortex (x=−36, y=−25, z=57), visual cortex (x=19, y=−98, z=−3), posterior cingulate cortex (x=0, y=−53, z=26), and medial prefrontal cortex (x=0, y=52, z=−6). These regions of interest have been previously used as control or experimental regions of interest in functional connectivity studies of aging (Hedden et al., 2009). There were no significant clusters associated with temporal discounting using any of these four seed regions of interest.

In order to clarify how our observations might support a particular model of temporal discounting, we conducted additional analyses using two 4mm-radius seed regions of interest in the dorsolateral prefrontal cortex (x=−44, y=36, z=20) and parahippocampal gyrus (x=24, y=−6, z=−30). Functional connectivity between the dorsolateral prefrontal cortex and fronto-insular regions was directly associated with temporal discounting (Figure 5, Table 3).

Functional connectivity between the parahippocampal gyrus and multiple regions in the frontal and temporal lobes was inversely associated with temporal discounting (Figure 6, Table 4).

Finally, we determined a median split in the population to examine if neural connections to the left FI differ between those exhibiting the highest and lowest degree of discounting. There were no demographic differences between median split groups (Table 5). Results showed that those with the lowest degree of discounting have greater connectivity of the FI to cerebellar and parahippocampal regions, and less connectivity to the caudate and precuneus regions (Figure 7, Table 6).

Discussion

In functional connectivity analyses adjusting for age, education, sex, and global cognition we observed a network of regions associated with temporal discounting in non-demented older adults. For our functional connectivity analyses, we utilized the fronto-insular cortex

(left and right) as our seed region of interest for three reasons: (1) it has been considered critical in studies of value-assessments and social decision making due to the proliferation of spindle neurons in this region (Allman et al., 2010), (2) it has been shown to be active during discounting tasks regardless of response (Whittman et al., 2010), suggesting it has an important role in decision making regardless of type of choice, and (3) it has been previously used to interrogate the functional network of frontal regions have been heavily implicated in studies of temporal discounting (Seeley et al., 2007). For the left FI region, temporal discounting was positively associated with functional connectivity to the right ventromedial prefrontal cortex and middle temporal regions, and negatively associated with functional connectivity to right parahippocampal and cerebellar regions. For the right FI region, temporal discounting was negatively associated with functional connectivity to the right cerebellum. In addition, functional connectivity maps separately associated with the left and right FI and temporal discounting appeared to overlap in a region of the right cerebellum. These observations appear to be selective to the FI as null findings were observed for four other seed regions of interest. Finally, a median split of the population by highest and lowest discounting showed functional connectivity differences to the FI, additionally supporting its importance for temporal discounting.

Previous task-related functional neuroimaging studies in younger adults have implicated a network of regions associated with temporal discounting, including the striatum, orbitofrontal cortex, ventromedial prefrontal cortex, anterior cingulate, insula, posterior cingulate, precuneus, angular gyrus, temporoparietal junction, and the inferior and middle temporal cortex (McClure et al., 2004; 2007; Hariri et al., 2006; Cardinal, 2001; Whittman et al., 2010). Theoretically, dorsolateral prefrontal and parietal networks process context information beyond and in conflict with limbic-striatal networks that presumably process the value of the immediate reward choice (McClure et al., 2004; 2007). This dualistic hypothesis therefore suggests that a network of brain regions is organized in two conflicting modules, one dedicated to the more rational cognitive processing of the delay reward benefit and the other dedicated more to immediate gratification (Christakou et al., 2011). Another hypothesis suggests that all of these regions are part of a unitary system that processes both immediate and delayed rewards with varying levels of activity across brain regions corresponding to different choices (Kable and Glimcher, 2007; 2010). A third and recent hypothesis of the neurobiological substrate of temporal discounting incorporates evidence from lesion studies that show hippocampal/parahippocampal lesions are associated with a preference for more immediate choices in rodents and humans (Peters and Buchel, 2010; 2011). This hypothesis proposes brain regions are organized in three subsystems: (1) a “valuation” subsystem consisting of the ventromedial prefrontal cortex, ventral striatum, insula and orbital frontal cortex (with the ventromedial prefrontal cortex as a hub); (2) a “cognitive control” subsystem consisting of the dorsolateral prefrontal cortex and anterior cingulate (with the anterior cingulate as a hub), and (3) an “imagery/prospection” subsystem consisting of medial temporal lobe structures. The imagery/prospection system is believed to assist in representations of a “future self”, and in the context of temporal discounting, this subsystem may assist with projection of the future self with the greater delayed reward. While our results may be viewed as generally consistent with the first hypothesis that proposes the notion of opposing subsystems (McClure et al., 2004; 2007), our results may be viewed as consistent with this third hypothesis of the neurobiological substrate of temporal discounting (Peters and Buchel, 2010; 2011) as we observed a direct association between discounting and connectivity to the ventromedial prefrontal cortex, and an inverse association between discounting and connectivity to parahippocampal regions for the left FI.

In order to more strongly test which model of temporal discounting might be most supported by our results, we conducted post-hoc analyses with two additional seed regions of interest in the dorsolateral prefrontal cortex and the parahippocampal gyrus. The first model of

temporal discounting proposes a subnetwork consisting of dorsolateral prefrontal and parietal regions at odds with a limbic-striatal subnetwork (McClure et al., 2004; McClure et al., 2007). Under this model, we would have expected to see an inverse relationship between the dorsolateral prefrontal cortex and limbic-striatal networks. This was not observed. Instead, dorsolateral prefrontal connectivity was associated with fronto-insular connectivity when considering temporal discounting, further supporting our use of the fronto-insular region as a seed region of interest. A second model of temporal discounting proposes that all brains regions that have been implicated in temporal discounting are part of a unitary system (Kable and Glimcher, 2007; Kable and Glimcher, 2010). Under this model, we would expect to see all of these regions functionally connected to our seed regions of interest. This was not observed. A third model proposes that memory networks are important for temporal discounting (Peters and Buchel, 2010; 2011). When seeding the right parahippocampal gyrus, we observed numerous and large significant clusters in frontal and temporal regions inversely related to temporal discounting. These results suggest functional connectivity of the parahippocampal gyrus is important for making better choices when given a temporal discounting option in older participants. Because of this, we conclude that our results most support the third model of temporal discounting (Peters and Buchel, 2010; 2011).

There have been some recent studies of temporal discounting in old age using behavioral and activity-based event-related fMRI measures. Eppinger et al. (2011) studied 17 younger adults and 15 older adults and found age-related reductions in temporal discounting. Furthermore, these older-age reductions in temporal discounting were associated with lower activity in ventral striatal regions. Samanez-Larkin et al. (2012) studied 12 younger adults and 13 older adults using similar methods and also found ventral striatum activity less strongly associated with temporal discounting in old age. Our results may be viewed as consistent with these findings in the sense that we did not see ventral striatal regions associated with the range of temporal discounting choices in our older age cohort. Since ventral striatal activity has been associated with immediate reward dopaminergic activity, and dopaminergic systems support associative learning about future rewards, the authors suggested there might be some degree of dopaminergic neuromodulation that occurs with age. Further research is needed to examine this hypothesis.

Resting-state fMRI was recently used to study temporal discounting in a young adult cohort. Li et al. (2013) studied 23 young adults and implicated four networks of brain regions: a network associated with money magnitude (right ventromedial prefrontal cortex, right striatum, right posterior cingulate cortex, right hippocampus, bilateral parahippocampal regions); a network associated with time delay (left anterior prefrontal cortex, left superior frontal gyrus, left dorsolateral prefrontal cortex, left inferior frontal gyrus, bilateral ventromedial prefrontal cortex, left dorsomedial prefrontal cortex, left inferior parietal lobe); and two networks related to the contrasts of hard and easy trials, a frontoparietal network (bilateral anterior prefrontal cortex, dorsolateral prefrontal cortex, inferior frontal gyrus, inferior parietal lobe, right superior frontal gyrus, right middle frontal gyrus); and a dorsal anterior cingulate-bilateral anterior insular cortex network. The authors additionally presented evidence that functional connectivity values between regions may predict temporal discounting in a separate sample. Our results show consistency with this study in terms of implicating the ventromedial prefrontal cortex and the parahippocampal gyrus as important for temporal discounting in old age. A notable difference between our study and that of Li et al. (2013) is in number of implicated regions. It is remarkable that studies of different age groups (e.g., Eppinger et al., 2011; Samenez-Larkin et al., 2012) using activity-based event-related fMRI suggest some brain regions important for temporal discounting choices in younger age may not be as active in old age (e.g., ventral striatum). Longitudinal paradigms are needed to explore whether this may be true for other brain regions.

The cerebellum has been increasingly implicated in complex cognitive control and behavior processing beyond motor movement (Buckner et al., 2011; Rapoport et al., 2000), and the right cerebellum in particular has been implicated in more verbal-oriented cognitive processing. Given that cerebellar regions are connected to contralateral regions in the cortex, it is notable that bilateral seed regions of interest from the left and right hemisphere converged in this right cerebellar region. The modality of our temporal discounting task was verbal in nature, which may be why we observed the right cerebellum as significant in our results. Conceptualization of the cerebellum's role in cognition and behavior is at an early stage; however, one formulation is that the cerebellum is involved in "predicting and preparing function" since it has diverse and integrative anatomical connections with cortical regions throughout the brain (Gottwald et al., 2004). This formulation is congruent with the implications of the presently observed findings suggesting this region in the right cerebellum may have an important function in temporal discounting choices in old age.

These results have implications for understanding temporal discounting and decision making in old age. Multiple studies have shown reduced or aberrant functioning of networks involving hippocampal/parahippocampal regions as an early sign of the dementia process (Buckner et al., 2005; Greicius et al., 2004). If this three-subsystem theory of temporal discounting is valid, then as the imagery/projection subsystem may functionally deteriorate, older adults may temporally discount more because of a weakening impact of the imagery/projection subsystem upon the valuation subsystem. However, this is speculation and needs to be experimentally tested with longitudinal models.

It should be noted that some groups have cautioned against interpretation of negative or inverse functional connectivity values because of methodological factors that may exaggerate negative or inverse findings (Van Dijk et al., 2010). We have chosen to present all data results in the effort of full disclosure to let the reader and other groups reflect upon the potential significance, if any, of these findings. In a dynamic, connectionist network model of brain connectivity, it is certainly conceivable that strengthening of some connections may be associated with weakening of others, as in the case of adolescent synaptic brain development where the outcome of synaptic pruning is presumably a more efficient system (Blakemore & Robbins, 2012). However, these general premises are outside the testable scope of the present study.

Limitations of the current study include the selected nature of the cohort and the fact that the questions used to ascertain temporal discounting involved hypothetical payments and not real monetary gains. However, studies have indicated that hypothetical temporal discounting situations show similar results to situations of real monetary gains. Using a within-subject design, Johnson and Bickel (2002) found that 5 out of 6 participants showed comparable rates of temporal discounting using a wide range of real and hypothetical monetary rewards. Locey et al. (2011) replicated this finding in a group of 150 participants who completed a paradigm that combined temporal discounting with the prisoner's dilemma. Bickel et al. (2009) extended these findings in thirty participants using functional MRI and again found no differences in the brain activation pattern elicited by real and hypothetical monetary rewards during a temporal discounting paradigm. These studies support the notion that real and hypothetical monetary rewards have comparable temporal discounting effects. Brevity of the temporal discounting assessment must also be acknowledged as a limitation, as a longer and more dynamic behavioral assessment of temporal discounting may have yielded more dynamic brain network characteristics and implicated more brain regions. Finally, the magnitude of rewards used in our measure of temporal discounting was relatively small. Others have noted that temporal discounting rates reduce with greater magnitudes of reward (Myerson et al., 2011; Ballard and Knutson, 2009; Johnson and Bickel, 2002). Therefore the magnitude of reward must be acknowledged as a limitation as we may have seen a larger

range of temporal discounting responses and neuroimaging results with a larger range in the magnitude of reward.

Strengths of the current study include the use of participants from a community-based epidemiologic study and the ability to adjust for multiple confounding factors such as age, education, sex, and global cognition that may have an impact upon functional connectivity analyses. Greater knowledge of brain networks and regions associated with temporal discounting in old age may have a significant public health impact by assisting in the development of interventions for poor decision making. Future research is needed to clarify what role each of these regions plays in decision making in old age.

Acknowledgments

This research was supported by National Institute on Aging grants R01AG17917, R01AG33678, K23AG40625, the American Federation for Aging Research, the Illinois Department of Public Health, and The Marsha K. Dowd Philanthropic Fund. The authors gratefully acknowledge the assistance of Dr. Randy Buckner, Dr. Gary Glover, and Dr. Jeffrey Rosengarten with this project. We thank Niranjini Rajendran, MS, and Woojeong Bang, MS, for image post-processing and statistical analyses. We also thank the Rush Memory and Aging Project staff and participants.

References

1. Ainslie G. Specious reward: A behavioral theory of impulsiveness and impulse control. Psychological Bulletin. 1975; 82:463–496. [PubMed: 1099599]
2. Allman JM, Tetreault NA, Hakeem AY, Manaye KF, Semendeferi K, Erwin JM, Park S, Goubert V, Hof PR. The von Economo neurons in frontoinsular and anterior cingulate cortex in great apes and humans. Brain Structure and Function. 2010; 214:495–517. [PubMed: 20512377]
3. Ballard K, Knutson B. Dissociable neural representations of future reward magnitude and delay during temporal discounting. NeuroImage. 2009; 45:143–150. [PubMed: 19071223]
4. Bennett DA, Schneider JA, Arvanitakis Z, Kelly JF, Aggarwal NT, Shah RC, et al. Neuropathology of older person without cognitive impairment from two community-based studies. Neurology. 2006; 27:1837–1844. [PubMed: 16801647]
5. Bennett DA, Wilson RS, Schneider JA, Evans DA, Beckett LA, Aggarwal NT, et al. Natural history of mild cognitive impairment in older persons. Neurology. 2002; 59:198–205. [PubMed: 12136057]
6. Bennett DA, Schneider JA, Buchman AS, Barnes LL, Boyle PA, Wilson RS. Overview and findings from the rush Memory and Aging Project. Curr Alzheimer Res. 2012; 9(6):646–663. [PubMed: 22471867]
7. Bickel WK, Miller ML, Yi R, Kowal BP, Lindquist DM, Pitcock JA. Behavioral and neuroeconomics of drug addiction: Competing neural systems and temporal discounting processes. Drug and Alcohol Dependence. 2007; 908:S85–S91. [PubMed: 17101239]
8. Bickel WK, Pitcock JA, Yi R, Angtuago Edgardo JC. Congruence of BOLD Response across Intertemporal Choice Conditions: Fictive and Real Money Gains and Losses: Behavioral and Neural Differences in Discounting. J Neurosci. 2009; 29:8839–8846. [PubMed: 19587291]
9. Blakemore S-J, Robbins TW. Decision-making in the adolescent brain. Nature Neuroscience. 2012; 15:1184–1191.
10. Boyle PA, Wilson RS, Aggarwal NT, Arvanitakis Z, Kelly J, Bienias JL, Bennett DA. Parkinsonian signs in subjects with mild cognitive impairment. Neurology. 2005; 65:1901–1906. [PubMed: 16380610]
11. Boyle PA, Yu L, Segawa E, Wilson RS, Buchman AS, Laibson DI, Bennett DA. Association of cognition with temporal discounting in community based older persons. BMC Geriatrics. 2012; 12:48. [PubMed: 22938391]
12. Buckner RL, Krienen FM, Castellanos A, Diaz JC, Yeo BTT. The organization of the human cerebellum estimated by intrinsic functional connectivity. J Neurophysiology. 2011; 106:2322–2345.

13. Buckner RL, Sepulcre J, Talukdar T, Krienen FM, Liu H, Hedden T, et al. Cortical hubs revealed by intrinsic functional connectivity: Mapping, assessment of stability, and relation to Alzheimer's disease. The Journal of Neuroscience. 2009; 29:1860–1873. [PubMed: 19211893]
14. Buckner RL, Synder AZ, Shannon BJ, LaRossa G, Sachs R, Fotenos AF, Sheline YI, Klunk WE, Mathis CA, Morris JC, Mintun MA. Molecular, structural, and functional characterization of Alzheimer's disease: Evidence for a relationship between default activity, amyloid, and memory. J Neurosci. 2005; 25:7709–7717. [PubMed: 16120771]
15. Cardinal RN, Pennicott DR, Sugathapala CL, Robbins TW, Everitt BJ. Impulsive choice induced in rats by lesions of the nucleus accumbens core. Science. 2001; 292:2499–2501. [PubMed: 11375482]
16. Christakou A, Brammer M, Rubia K. Maturation of limbic corticostriatal activation and connectivity associated with developmental changes in temporal discounting. NeuroImage. 2011; 54:1344–1354. [PubMed: 20816974]
17. Eppinger B, Nystrom LE, Cohen JD. Reduced sensitivity to immediate reward during decision-making in older than younger adults. Plos One. 2012; 7(5):e36953. [PubMed: 22655032]
18. Frederick S, Loewenstein G, O'Donoghue T. Time discounting and time preference: a critical review. J Econ Lit. 2002; 40:351–401.
19. Gottwald B, Wilde B, Mihajlovic Z, Mehdorn HM. Evidence for distinct cognitive deficits after focal cerebellar lesions. JNNP. 2004; 75:1524–1531.
20. Greicius MD, Srivastava G, Reiss AL, Menon V. Default-mode network activity distinguishes Alzheimer's disease from healthy aging: Evidence from functional MRI. Proc Natl Acad Sci. 2004; 101:4637–4642. [PubMed: 15070770]
21. Hariri AR, Brown SM, Williamson DE, Flory JD, de Wit H, Manuck SB. Preference for immediate over delayed rewards is associated with magnitude of ventral striatal activity. J Neuroscience. 2006; 26:13213–13217.
22. Johnson MW, Bickel WK. Within-subject comparison of real and hypothetical money rewards in delay discounting. Journal of the Experimental Analysis of Behavior. 2002; 77:129–146. [PubMed: 11936247]
23. Kable JW, Glimcher PW. The neural correlates of subjective value during intertemporal choice. Nat Neuroscience. 2007; 10:1625–1633.
24. Kable JW, Glimcher PW. An "as soon as possible" effect in human inter-temporal decision making: Behavioral evidence and neural mechanisms. J Neurophysiology. 2010; 103:2513–2531.
25. Kirby KN. Bidding on the future: evidence against normative discounting of delayed rewards. J Exp Psychol. 1997; 126(1):54–70.
26. Kirby KN, Petry NM, Bickel WK. Heroin addicts have higher discount rates for delayed rewards than non-drug-using controls. J Exp Psychol. 1999; 128:78–87.
27. Kishinevsky FI, Cox JE, Murdaugh DL, Stoeckel LE, Cook EW, Weller RE. fMRI reactivity on a delay discounting task predicts weight gain in obese women. Appetite. 2012; 58:582–592. [PubMed: 22166676]
28. Laibson D. Life-cycle consumption and hyperbolic discount functions. European Economic Review Papers and Proceedings. 1998; 42(3–5):861–871.
29. Laibson D. Golden eggs and hyperbolic discounting. Q J Econ. 1997; 112:443–478.
30. Li N, Ma N, Liu Y, He XS, Sun DL, Fu XM, Zhang X, Han S, Zhang DR. Resting-state functional connectivity predicts impulsivity in economic decision-making. Journal of Neuroscience. 2013; 33(11):4886–4895. [PubMed: 23486959]
31. Locey ML, Jones BA, Rachlin H. Real and hypothetical rewards. Judg Decis Mak. 2011; 6:552–564.
32. McClure SM, Ericson KM, Laibson DI, Loewenstein G, Cohen JD. Time discounting for primary rewards. Journal of Neuroscience. 2007; 27:5796–5804. [PubMed: 17522323]
33. McClure SM, Laibson DI, Loewenstein G, Cohen JD. Separate neural systems value immediate and delayed monetary rewards. Science. 2004; 306:503–507. [PubMed: 15486304]
34. Meier S, Sprenger C. Present-Biased Preferences and Credit Card Borrowing. American Economic Journal: Applied Economics. 2010; 2(1):193–210.

35. Myerson J, Green L, Morris J. Modeling the Effect of Reward Amount on Probability Discounting. J Exp Anal Behav. 2011; 95(2):175–187. [PubMed: 21541126]

36. Peters J, Buchel C. Episodic future thinking reduces reward delay discounting through and enhancement of prefrontal-mediotemporal interactions. Neuron. 2010; 66:138–148. [PubMed: 20399735]

37. Peters J, Buchel C. The neural mechanisms of inter-temporal decision-making: understanding variability. Trends in Cognitive Science. 2011; 15:227–239.

38. Rapoport M, van Reekum R, Mayberg H. The role of the cerebellum in cognition and behavior: A selective review. The Journal of Neuropsychiatry. 2000; 12:193–198.

39. Samanez-Larkin GR, Mata R, Radu PT, Ballard IC, Carstensen LL, McClure SM. Age differences in striatal delay sensitivity during intertemporal choice in healthy adults. Frontiers in Neuroscience. 5:126. [PubMed: 22110424]

40. Seeley WW, Menon V, Schatzberg AF, Keller J, Glover GH, Kenna H, Reiss AL, Greicius MD. Dissociable intrinsic connectivity networks for salience processing and executive control. Journal of Neuroscience. 2007; 28:2349–2356. [PubMed: 17329432]

41. Shih P, Shen M, Ottl B, Keehn B, Gaffrey MS, Muller R-A. Atypical network connectivity for imitation in autism spectrum disorder. Neuropsychologia. 2010; 48:2931–2939. [PubMed: 20558187]

42. Van Dijk KRA, Hedden T, Venkataraman A, Evans KC, Lazar SW, Buckner RL. Intrinsic functional connectivity as a tool for human connectomics: Theory, properties, and optimization. J Neurophysiol. 2010; 103:297–321. [PubMed: 19889849]

43. Whittman M, Lovero KL, Lane SD, Paulus M. Now or later? Striatum and insula activation to immediate versus delayed rewards. Journal of Neuroscience, Psychology, and Economics. 2010; 3:15–26.

HIGHLIGHTS

- We correlated temporal discounting choices with resting-state fMRI in older adults.
- Ventromedial prefrontal cortex connectivity correlated directly with discounting.
- Parahippocampal gyrus connectivity correlated inversely with discounting.
- Results implicate brain networks important for decision making in old age.

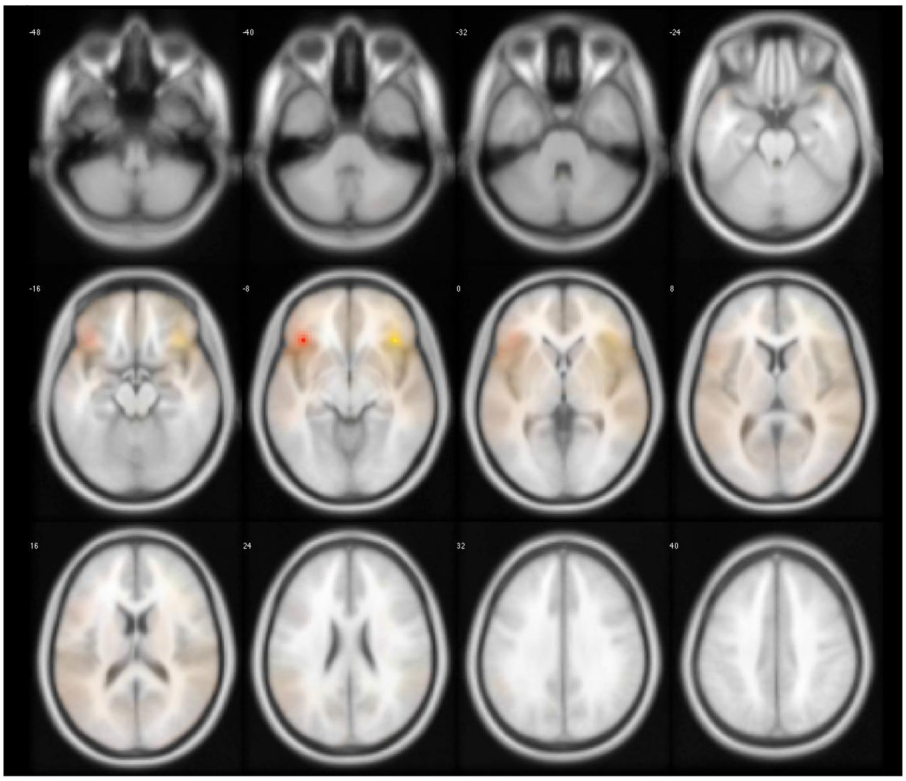

Figure 1.
Whole-brain rendering of functionally connected voxels to the left (red shading) and right (yellow shading) fronto-insular (FI) cortex seed regions of interest (ROIs). AlphaSim Monte Carlo simulation corrected for multiple comparisons at cluster $p<0.05$, cluster size > 39 voxels, voxel threshold $p<0.004$ for the left FI and right FI.

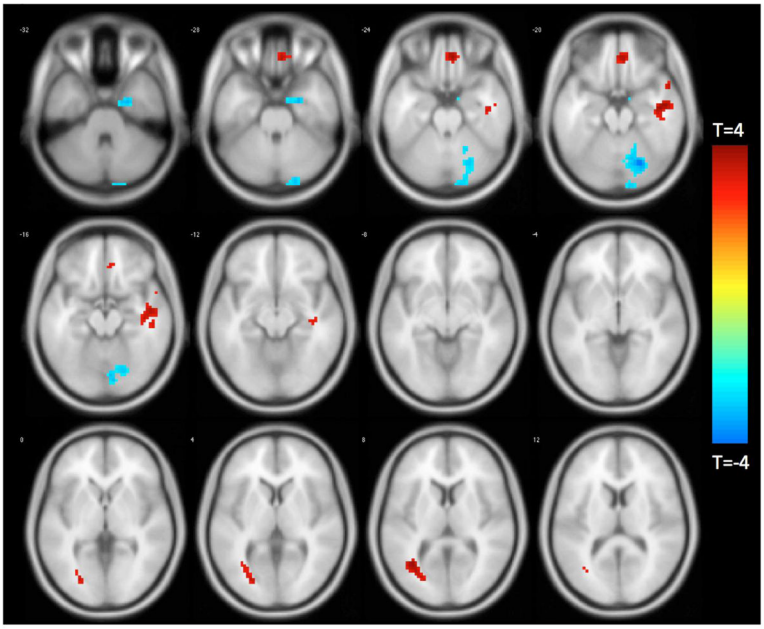

Figure 2.
Functionally connected clusters associated with temporal discounting after adjusting for age, education, sex, and global cognition, as indicated by a seed region of interest (ROI) prescribed in the left fronto-insular cortex. Seed ROI MNI coordinates: x = −38, y = 26, z = −10; radius = 4 mm; $p < 0.004$; cluster size > 39 voxels. Corrected for multiple comparisons using AlphaSim Monte Carlo simulations at a cluster level threshold of $p<0.05$. Values shown in scale correspond to t-scores.

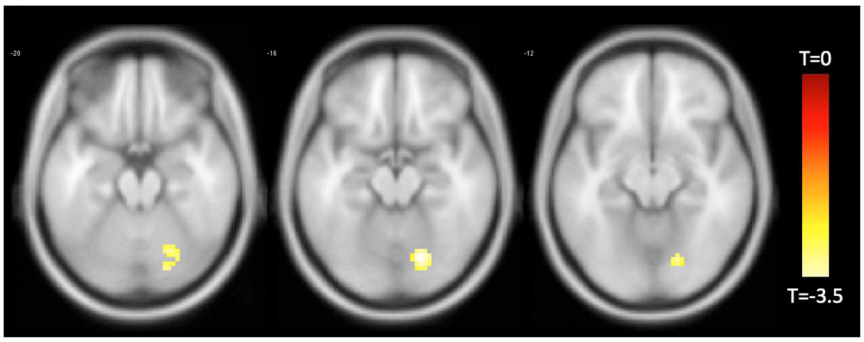

Figure 3.
Functionally connected clusters associated with temporal discounting after adjusting for age, education, sex, and global cognition, as indicated by a seed region of interest (ROI) prescribed in the right fronto-insular cortex. Seed ROI MNI coordinates: x = 38, y = 26, z = −10; radius = 4 mm; $p < 0.004$; cluster size > 39 voxels. Corrected for multiple comparisons using AlphaSim Monte Carlo simulations at a cluster level threshold of $p<0.05$. Values shown in scale correspond to t-scores.

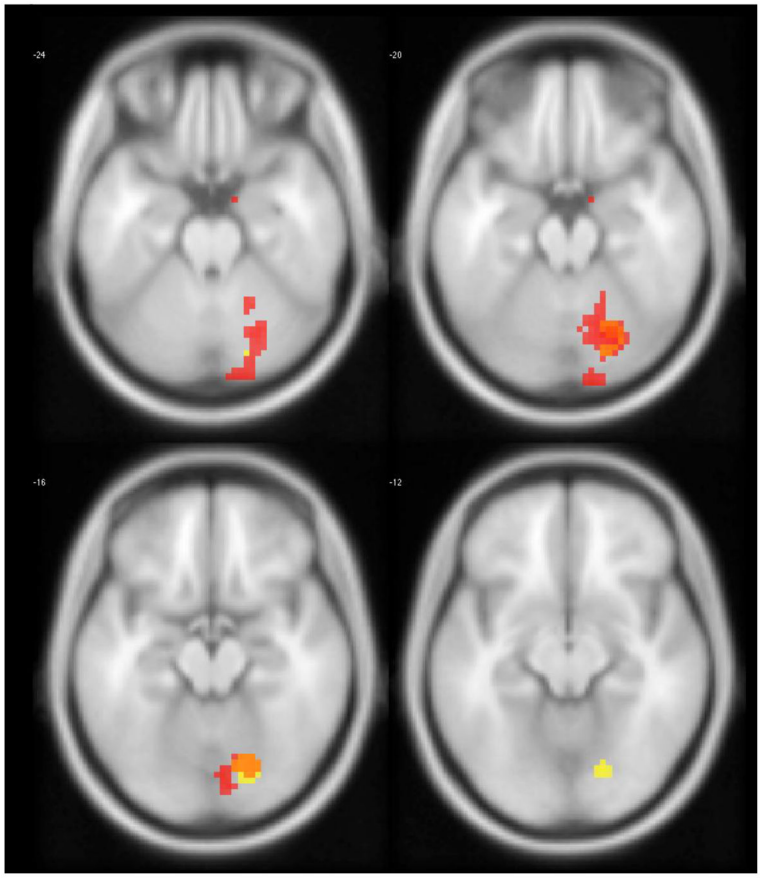

Figure 4.
Statistically significant clusters associated with temporal discounting indicated by a seed region of interest (ROI) prescribed in the left (reds) and right (yellows) fronto-insular cortex. Overlap between both seeds can be seen in orange voxels in the right cerebellum.

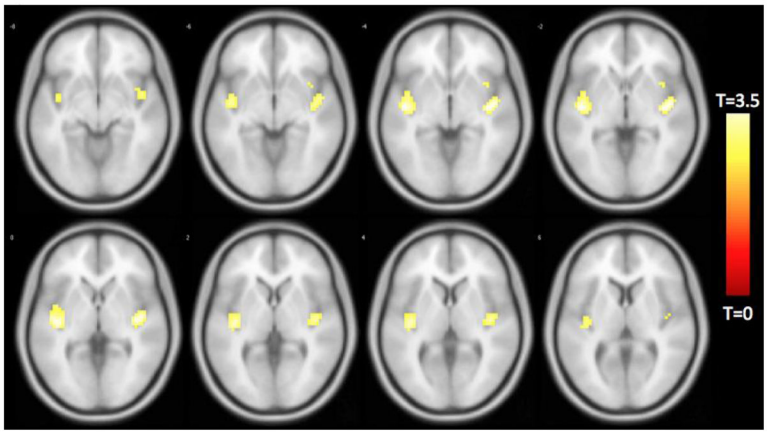

Figure 5.

Functionally connected clusters associated with temporal discounting after adjusting for age, education, sex, and global cognition, as indicated by a seed region of interest (ROI) prescribed in the left dorsolateral prefrontal cortex. Seed ROI MNI coordinates: x = −44, y = 36, z = 20; radius = 4 mm; $p < 0.004$; cluster size > 39 voxels. Corrected for multiple comparisons using AlphaSim Monte Carlo simulations at a cluster level threshold of $p<0.05$. Values shown in scale correspond to t-scores.

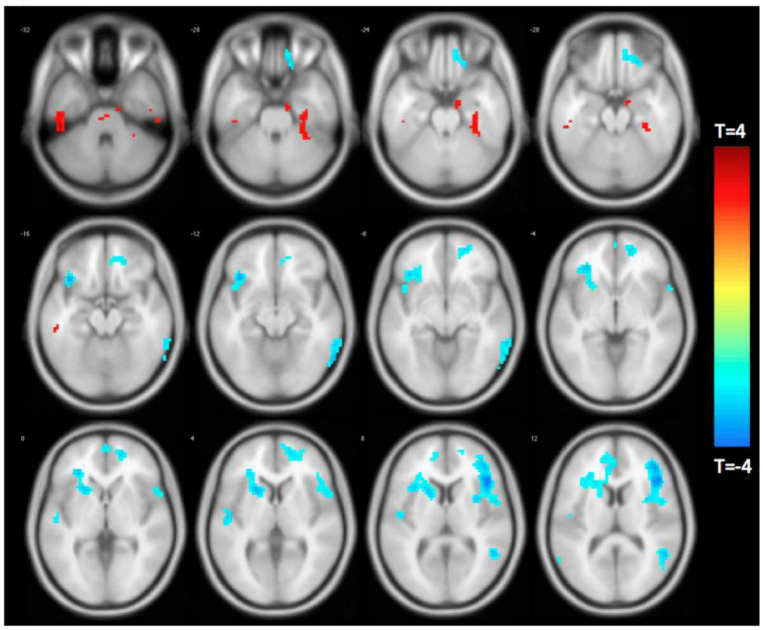

Figure 6.
Functionally connected clusters associated with temporal discounting after adjusting for age, education, sex, and global cognition, as indicated by a seed region of interest (ROI) prescribed in the ventromedial prefrontal cortex. Seed ROI MNI coordinates: x = 24, y = −6, z = 30; radius = 4 mm; $p < 0.004$; cluster size > 39 voxels. Corrected for multiple comparisons using AlphaSim Monte Carlo simulations at a cluster level threshold of $p<0.05$. Values shown in scale correspond to t-scores.

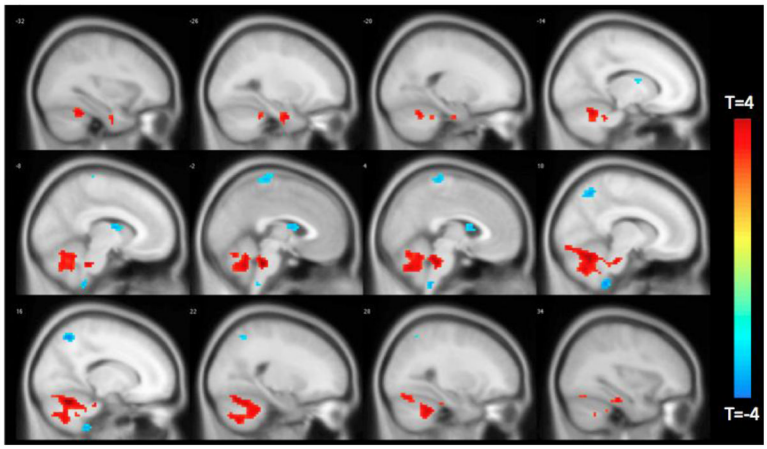

Figure 7.
Difference in functionally connected clusters to the left FI according to median split of participants by temporal discounting response. Positive (red) clusters are those significantly more connected to left FI in the low discounting group. Negative (blue) clusters are those significantly less connected to left FI in the low discounting group.

Table 1

Statistics for demographic and cognitive variables for the sample

	Total sample (*n* = 123)
Age (years)	
Mean (*SD*)	82.95 (6.64)
Range	60 – 98
Education (years)	
Mean (*SD*)	15.67 (3.20)
Range	10 – 28
Sex (% Female)	82.1% (*n* = 101)
Race (% White)	100% (*n* = 123)
MMSE (total score)	
Mean (*SD*)	28.49 (1.57)
Range	23 – 30
Global Cognition Z-score	
Mean (*SD*)	0.37 (0.50)
Range	−1.78 – 1.47
Alpha (temporal discounting)	
Mean (*SD*)	0.015 (0.020)
Range	0.0023 – 0.0867

Note: Data are summarized as Mean (standard deviation = *SD*), unless otherwise indicated.

Exp Gerontol. Author manuscript; available in PMC 2014 December 01.

Table 2

Functionally connected clusters associated with temporal discounting, as indicated by a seed region of interest (ROI) prescribed in the left and right fronto-insular cortex, adjusting for age, education, sex, and global cognition

Seed ROI	Region of Maximum Intensity Voxel	Maximum Intensity Voxel Coordinates (MNI)			Cluster Size (# of voxels)	t-value
		X	Y	Z		
Left FI						
	R parahippocampal	24	−6	−30	46	−3.7129
	R cerebellum	24	−72	−21	204	−4.1652
	R ventromedial prefrontal	6	42	−24	53	3.7059
	R middle temporal	51	−9	−18	120	3.9395
	L temporal-occipital	−36	−63	9	81	3.7381
Right FI						
	R cerebellum	18	−69	−18	69	−3.8735

Table 3

Functionally connected clusters associated with temporal discounting, as indicated by a seed region of interest (ROI) prescribed in the dorsolateral prefrontal cortex, adjusting for age, education, sex, and global cognition

Seed ROI	Region of Maximum Intensity Voxel	Maximum Intensity Voxel Coordinates (MNI)			Cluster Size (# of voxels)	t-value
		X	Y	Z		
L dorsolateral						
	R fronto-insular	42	−12	−3	103	3.8405
	L fronto-insular	−45	−12	−3	122	3.9534

Table 4

Functionally connected clusters associated with temporal discounting, as indicated by a seed region of interest (ROI) prescribed in the right parahippocampal cortex, adjusting for age, education, sex, and global cognition

Seed ROI	Region of Maximum Intensity Voxel	Maximum Intensity Voxel Coordinates (MNI)			Cluster Size (# of voxels)	t-value
		X	Y	Z		
R parahippocampal						
	R inferior temporal	18	−12	−42	258	4.6316
	L inferior temporal	−48	−33	−33	64	3.9838
	R cerebellum	30	−42	−30	61	3.3932
	R inferior frontal	45	24	9	530	−4.6896
	R middle temporal	63	−60	−12	70	−3.8465
	L fronto-insular	−39	24	−12	465	−4.2708
	L superior temporal	−48	−12	6	39	−3.5014
	R middle temporal	51	−54	12	319	−3.7293
	L angular	−48	−69	30	55	−3.3928
	L precentral	−45	0	21	102	−3.8989
	L postcentral	−24	−42	39	44	4.2317

Table 5

Statistics for demographic and cognitive variables for the median split samples

	Low Alpha (*n* = 61)	**High Alpha (*n* = 62)**
Age (years)		
Mean (*SD*)	83.51 (6.22)	82.39 (7.03)
Education (years)		
Mean (*SD*)	16.13 (3.59)	15.23 (2.73)
Sex (% Female)	75.4% (*n* = 46)	88.7% (*n* = 55)
Race (% White)	100% (*n* = 61)	100% (*n* = 62)
MMSE (total score)		
Mean (*SD*)	28.66 (1.60)	28.33 (1.52)
Global Cognition Z-score		
Mean (*SD*)	0.45 (0.48)	0.29 (0.52)

Note: Data are summarized as Mean (standard deviation = *SD*), unless otherwise indicated.

Exp Gerontol. Author manuscript; available in PMC 2014 December 01.

Table 6

Difference in functionally connected clusters to the left FI according to median split of participants by temporal discounting response. Positive clusters are those significantly more connected to left FI in the low discounting group. Negative clusters are those significantly less connected to left FI in the low discounting group

Seed ROI	Region of Maximum Intensity Voxel	Maximum Intensity Voxel Coordinates (MNI)			Cluster Size (# of voxels)	t-value
		X	Y	Z		
L FI						
	R cerebellum	6	−42	−60	82	−4.1444
	R cerebellum	15	−60	−24	1248	4.7772
	L parahippocampal	−30	−6	−33	46	3.6991
	L caudate	0	6	12	67	−3.3793
	R precuneus	12	−60	54	72	−3.8791
	Paracentral lobule	0	−30	72	57	−3.3327

Exp Gerontol. Author manuscript; available in PMC 2014 December 01.